Journal of Alloys and Compounds, 194 (1993) 87–91
JALCOM 548

Intrinsic and hard magnetic properties of rapidly quenched $NdFe_{10}Mo_2N_x$ ribbons

Z. X. Tang and G. C. Hadjipanayis
Department of Physics and Astronomy, University of Delaware, Newark, DE 19716 (USA)

V. Papaefthymiou
Department of Physics, University of Ionniana, Ionniana (Greece)

(Received August 24, 1992; in final form September 23, 1992)

Abstract

The magnetic anisotropy fields of nitrogenated $NdFe_{10}Mo_2N_x$ compound are found to be 20 and 8.6 T at 10 and 300 K respectively. Magnetically hard $NdFe_{10}Mo_2N_x$ with a coercivity of 8.8 kOe at room temperature and 33.7 kOe at 10 K is obtained by nitrogenating melt-spun $NdFe_{10}Mo_2$ ribbons. The coercivity depends strongly on the nitrogenation temperature and time with the maximum values obtained for nitrogenation at 570 °C for 4 h. The high coercivity is related to the purity of the $ThMn_{12}$ phase and the uniformity of nitrogenation.

1. Introduction

Rare earth–transition metal compounds with the $ThMn_{12}$ crystal structure have a small rare earth fraction. Their potential as permanent magnets has been exploited [1–3]. Wang and Hadjipanayis [4] obtained a coercivity of 10.7 kOe in rapidly quenched $Sm_8Fe_{75.5}Ga_{0.5}Ti_8V_8$ and similar results in other Sm–Fe-based compositions. Unfortunately, only $Sm(Fe, M)_{12}$ (where M is another transition metal) has sufficiently high magnetocrystalline anisotropy. This causes problems because of the scarcity of Sm. Therefore it is desirable to substitute Sm by other rare earth elements and to retain the high uniaxial anisotropy. Nitrogenation in the gas phase [5, 6] has been successfully used to fulfil this requirement [7–10]. Wang *et al.* [9, 10] have observed uniaxial anisotropy in $RFe_{10}V_2N_x$, where $R \equiv Y$, Nd, Gd, Dy and Er. In contrast, $SmFe_{10}V_2N_x$ has a planar anisotropy. The magnetic properties, including the hard magnetic properties, have also been investigated. Anagnostou *et al.* [11] have studied the intrinsic properties of $NdFe_{10}Mo_2N_x$ and $NdFe_{10}V_2N_x$ compounds. Mechanically alloyed $Nd_{10}Fe_{75}Mo_{15}N_x$ powders show a coercivity of 4.5 kOe [12] and 8 kOe [13]. In addition, a coercivity of 5 kOe [14] in $NdFe_{10}V_2$ ribbons has been obtained using melt spinning. In this work, we have prepared magnetically hard $NdFe_{10}Mo_2N_x$ samples with a coercivity of 8.8 kOe at room temperature and 33.7 kOe at 10 K by nitrogenating melt-spun $NdFe_{10}Mo_2$ ribbons.

2. Experimental details

Alloys with the composition $NdFe_{10}Mo_2$ were prepared by arc melting using materials of 99.9% purity. Powder samples were obtained by homogenizing the alloys at 1050 °C for 48 h, followed by pulverizing to a particle size of less than 45 μm. Rapidly quenched ribbons were produced by melt spinning the alloys with a wheel speed of 40 m s^{-1}. The ribbons were vacuum annealed to optimize the grain size and then pulverized to a particle size of less than 45 μm. Samples were nitrogenated with N_2 gas above 500 °C.

Powder X-ray diffraction patterns were obtained using a Philips PW 1710 diffractometer with Cu Kα radiation. The diffraction experiments were performed on both random and oriented powders. The easy magnetization direction (EMD) was deduced from the diffraction patterns of powders which were aligned in a magnetic field of 10 kOe. The magnetic measurements were made with a superconducting quantum interference device (SQUID) magnetometer in magnetic fields up to 5.5 T below room temperature and with a vibrating sample magnetometer (VSM) in fields up to 1.5 T above room temperature.

The Mössbauer spectra were taken with a conventional transmission spectrometer with a γ-ray source of ^{57}Co embedded in an Rh matrix. The isomer shifts are given relative to α-Fe at room temperature. The analysis of the spectra into the components was carried out assuming a distribution of hyperfine fields in each

0925-8388/93/$6.00

subcomponent and using standard least-squares fitting techniques.

3. Results and discussion

3.1. Intrinsic properties of $NdFe_{10}Mo_2$

Figure 1 shows the X-ray diffraction patterns of $NdFe_{10}Mo_2$ before and after nitrogenation at 570 °C for 4 h. Ribbon samples show the same results. The X-ray diffraction peaks were indexed in accordance with the $ThMn_{12}$ structure. The structural properties derived from X-ray diffraction are listed in Table 1. The lattice constants a and c and therefore the volume of the unit cell (V) of both powders and ribbons increase significantly due to the introduction of nitrogen into the lattice. The increase in the unit cell volume by nitrogenation is about 3%.

The intrinsic magnetic properties of the nitrides obtained via nitrogenation and their corresponding nitrogen-free compounds are listed in Table 2. The Curie temperatures were determined by thermomagnetic curves in an external magnetic field of 400 Oe. The Curie temperature increases by 197 K after nitrogenation to 563 K. The spontaneous magnetization (M_s) data were derived by extrapolating the high-field (30–55 kOe) part of the M (H) curves to zero field. Interstitial nitrogen addition increases the spontaneous magnetization. At 10 K, M_s increases by about 15%, whereas at room temperature, the spontaneous magnetization increases drastically by 55%, mainly because of the low Curie temperature (366 K) of the parent compound.

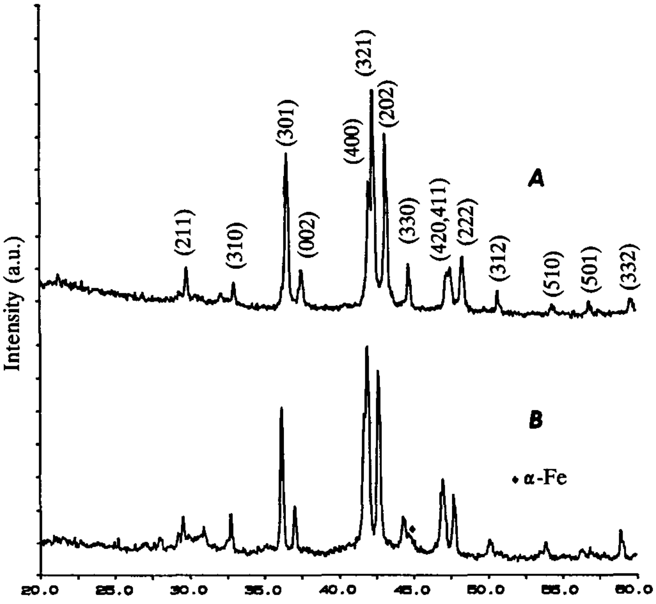

Fig. 1. X-ray diffraction patterns of $NdFe_{10}Mo_2$ powders before (A) and after (B) nitrogenation at 570 °C for 4 h.

TABLE 1. Structural properties of $NdFe_{10}Mo_2$ powders and ribbons before and after nitrogenation (the data in parentheses pertain to the nitrides)

Property	Powders ($ThMn_{12}$)	Ribbons ($ThMn_{12}$)
a (nm)	0.860 (0.866)	0.858 (0.865)
c (nm)	0.480 (0.486)	0.479 (0.487)
V (nm^3)	0.355 (0.365)	0.353 (0.364)
$\Delta V/V_0$ (%)	(2.8)	(3.4)

TABLE 2. Intrinsic properties of $NdFe_{10}Mo_2$ powders before and after nitrogenation

Property	Before	After
T_c (K)	366	563
ΔT_c (K)		197
M_s (10 K) (e.m.u. g^{-1})	85.5	98.7
M_s (300 K) (e.m.u. g^{-1})	51.6	80.2
EMD	ab-plane	c-axis
H_a (10 K) (T)	2.0	20.0
H_a (300 K) (T)	1.0	8.6

The EMD was determined by X-ray diffraction on magnetically aligned powders. The magnetic anisotropy field was obtained from the intersection of the magnetization curves measured parallel and perpendicular to the alignment direction. The nitrogen uptake changes the EMD from ab-plane to c-axis. For $NdFe_{10}Mo_2N_x$, the anisotropy field is equal to 20 and 8.6 T at 10 and 300 K respectively. These anisotropy fields are comparable with those of $Nd_2Fe_{14}B$ which are equal to 17 and 7.3 T at 4 and 295 K respectively [15].

3.2. Hyperfine interactions

The effects of nitrogenation were also studied by Mössbauer spectroscopy in the temperature range 20–300 K. Figure 2 shows typical Mössbauer spectra for $NdFe_{10}Mo_2$ ribbons before and after nitrogenation at 570 °C for 4 h. The spectra of the parent compounds can be decomposed into three subcomponents corresponding to the three iron sites in the $ThMn_{12}$ structure. The three subcomponents were assigned to the 8f, 8i and 8j sites of the $ThMn_{12}$ structure according to other results [16, 17]. After nitrogenation, another subcomponent which corresponds to α-Fe(Mo) appears. This component accounts for only 5% of the total iron atoms. As expected from the spontaneous magnetization measurements, the hyperfine magnetic fields are increased by nitrogenation. The effect is more enhanced at room temperature than at lower temperature, as observed for the change in the spontaneous magnetization, because of the lower Curie temperature of the parent

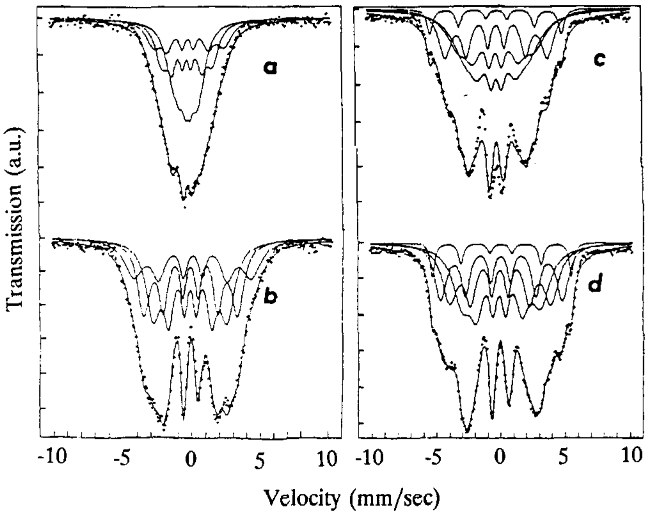

Fig. 2. Mössbauer spectra of ribbon samples: (a) $NdFe_{10}Mo_2$ at 295 K; (b) $NdFe_{10}Mo_2$ at 20 K; (c) $NdFe_{10}Mo_2N_{0.83}$ at 295 K; (d) $NdFe_{10}Mo_2N_{0.83}$ at 20 K.

compounds. The weighted average hyperfine fields of the nitrides are 237 and 188 kOe at 20 and 295 K respectively. These are 14% higher at 20 K and 44% higher at 295 K than those of the parent alloys.

3.3. Hard magnetic properties of $NdFe_{10}Mo_2N_x$

From the intrinsic magnetic properties, it is obvious that the anisotropy field (8.6 T at room temperature) and Curie temperature (563 K) of the nitrides are comparable with those of $Nd_2Fe_{14}B$ and Sm–Fe-based $ThMn_{12}$ magnets, indicating that they are suitable for permanent magnet development. However, the coercivity, one of the important application parameters, is an extrinsic property and is strongly dependent on the microstructure. In order to optimize the microstructure, the sample preparations discussed below were followed.

(a) Initially, the arc-melted alloys were melt spun to obtain nanocrystalline ribbons. It is not absolutely necessary to obtain the $ThMn_{12}$ phase at this step. However, ultrafine grain sizes are the key characteristics as a fine grain size will make it easy to grow the right phase in the later steps. In the case of $NdFe_{10}Mo_2$, the as-spun samples possess the $ThMn_{12}$ structure. Figure 3(A) shows the X-ray diffraction pattern for the as-spun $NdFe_{10}Mo_2$ sample. The fine grain size can be easily seen from the broad diffraction peaks.

(b) The rapidly quenched samples were vacuum annealed to optimize the grain size. The X-ray diffraction pattern for a sample annealed at 850 °C for 20 min is shown in Fig. 3(B). It exhibits a fairly pure $ThMn_{12}$ structure without any other phases, including free iron. The diffraction indices are marked in the graph. The optimized annealing temperature and time must be evaluated for the hard magnetic properties after nitrogenation.

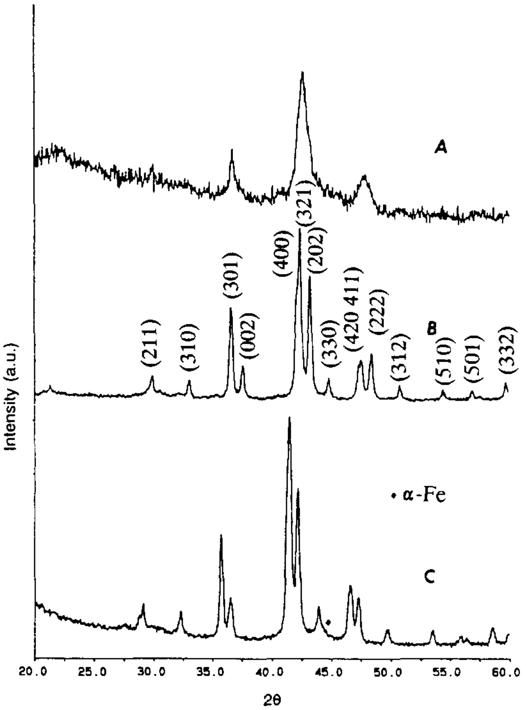

Fig. 3. X-ray diffraction patterns of $NdFe_{10}Mo_2$ ribbons: (A) as-spun; (B) vacuum annealed at 850 °C for 20 min; (C) nitrogenated at 570 °C for 4 h.

(c) The annealed samples were nitrogenated at an appropriate temperature and time to obtain uniform nitrides. X-ray diffraction shows that nitrogen gas enters the $ThMn_{12}$ structure by a gas–solid reaction at temperatures above 500 °C. The optimum temperature at which uniform nitrogenation can be obtained quickly without inducing free iron is found to be 570 °C. Figure 3(C) shows the X-ray diffraction pattern of the sample in Fig. 3(B) nitrogenated at 570 °C for 4 h. As in the bulk powder sample, the X-ray diffraction patterns of the original $ThMn_{12}$ phase are retained after nitrogenation, and show an obvious peak shift towards lower angles relative to the corresponding nitrogen-free phase, indicating a lattice expansion. The structural data of the ribbon samples are listed in Table 1.

It is worthwhile to describe the nitrogenation process in more detail. A common problem in the studies of interstitial-atom-modified rare earth–transition metal compounds is incomplete nitrogenation. The interstitial-atom-modified phase (nitride or carbide) is magnetically hard, while the parent phase is soft. Incomplete nitrogenation usually results in a "hard" shell and a "soft" core [18]. In order to obtain a high coercivity, this situation should be avoided as much as possible. The room temperature coercivities of $NdFe_{10}Mo_2N_x$ ribbons obtained after different nitrogenation times at 570 °C are listed in Table 3. The nitrogen-free sample has a coercivity of only 0.2 kOe. The coercivity increases steadily with increasing nitrogenation time. The coer-

TABLE 3. Room temperature coercivity of $NdFe_{10}Mo_2N_x$ ribbons obtained after different nitrogenation times at 570 °C

Nitrogenation time (h)	Coercivity (kOe)
0	0.2
1.5	1.3
3.2	4.0
4.0	8.8
10.7	7.5

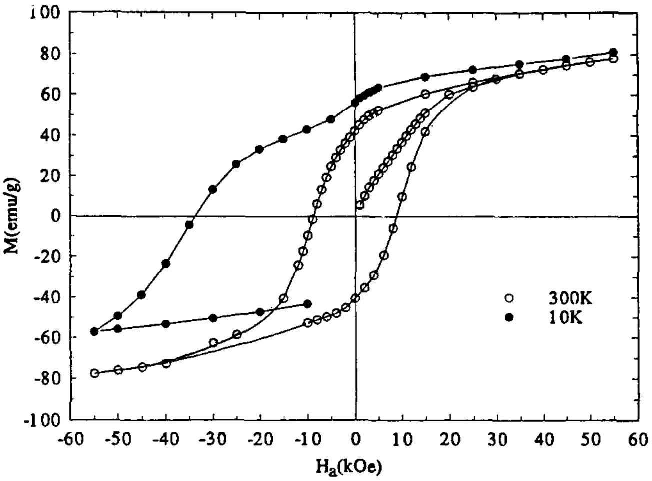

Fig. 4. Hysteresis loops of $NdFe_{10}Mo_2N_{0.83}$ ribbons at 10 and 300 K.

TABLE 4. Hard magnetic properties of $NdFe_{10}Mo_2N_{0.83}$ ribbons

Property	10 K	300 K
M_s (at 55 kOe, e.m.u. g^{-1})	82	79
M_r (e.m.u. g^{-1})	57	43
H_c (kOe)	33.7	8.8

civity reaches a maximum after 4 hours of nitrogenation. A further increase in the nitrogenation time produces a lower coercivity most probably because of the decomposition of the alloys into α-Fe and Nd–N. The nitrogenation process can be operated only in a narrow temperature and time region where the maximum uniformity of nitrogenation can be obtained without causing obvious decomposition.

Figure 4 shows the hysteresis loops of our high coercivity $NdFe_{10}Mo_2N_x$ sample at 10 and 300 K. The coercivity reaches 8.8 kOe at room temperature and 33.7 kOe at 10 K. The hard magnetic properties of this sample are summarized in Table 4. It seems that two factors are important for the high coercivity: the purity of the $ThMn_{12}$ phase and the uniformity of nitrogenation. Yelon and Hadjipanayis [19] studied the same sample using neutron diffraction and found only 5% of Fe present. The composition was determined to be $NdFe_{10}Mo_2N_{0.83}$ with more than 80% of the available 2b sites occupied by nitrogen atoms, indicating a fairly good uniformity of nitrogenation throughout the particles. The nitrogen content was higher than that of other observations [7, 8], which is usually $R(Fe,M)_{12}N_{0.5}$.

4. Conclusions

In summary, the interstitial nitrogen atoms introduced by nitrogenation in a nitrogen gas atmosphere expand the unit cell volume of $NdFe_{10}Mo_2$ by about 3%. After nitrogenation the Curie temperature of the nitride reaches 563 K, and the magnetic anisotropy field is 20 and 8.6 T at 10 and 300 K respectively, making this compound a prospective permanent magnet. Magnetically hard $NdFe_{10}Mo_2N_x$ with a coercivity of 8.8 kOe at room temperature and 33.7 kOe at 10 K is obtained by nitrogenating the melt-spun $NdFe_{10}Mo_2$ ribbons. The coercivity strongly depends on the nitrogenation temperature and time with a maximum at 570 °C for 4 h. The high coercivity is related to the purity of the $ThMn_{12}$ phase and the uniformity of nitrogenation. The $ThMn_{12}$ structure is retained after nitrogenation with only 5% of free iron as an impurity. The nitrogen content is very close to the saturation value, indicating fairly uniform nitrogenation throughout the particles.

Acknowledgments

This work was supported by DOE DE-FG02-90ER 45413 and a NATO Research Grant.

References

1 E. W. Singleton, J. Strzeszewski and G. C. Hadjipanayis, *Appl. Phys. Lett., 54* (1989) 1934.
2 J. Strzeszewski, Y. Z. Wang, E. W. Singleton and G. C. Hadjipanayis, *IEEE Trans. Magn., 25* (1989) 3309.
3 F. R. deBoer, Y. K. Huang, D. B. de Mooij and K. H. J. Buschow, *J. Less-Common Met., 135* (1987) 199.
4 Y. Z. Wang and G. C. Hadjipanayis, *J. Magn. Magn. Mater., 87* (1989) 375.
5 J. M. D. Coey and H. Sun, *J. Magn. Magn. Mater., 87* (1990) L251.
6 H. Sun, J. M. D. Coey, Y. Otani and D. P. F. Hurley, *J. Phys. C, 2* (1990) 6465.
7 Y. Yang, X. Zhang, L. Kong, Q. Pan and S. Ge, *Solid State Commun., 78* (1991) 313.
8 Y. Yang, X. Zhang, L. Kong, Q. Pan and S. Ge, *Appl. Phys. Lett., 58* (1991) 2042.
9 Y. Z. Wang and G. C. Hadjipanayis, *J. Appl. Phys., 70* (1991) 6009.

10 Y. Z. Wang, G. C. Hadjipanayis, A. Kim, D. J. Sellmyer and W. B. Yelon, *J. Magn. Magn. Mater.*, *104–107* (1992) 1132.

11 M. S. Anagnostou, C. Christides, M. Pissas and D. Niarchos, *J. Appl. Phys.*, *70* (1991) 15.

12 M. Endoh, K. Nakamura and H. Mikami, *IEEE Trans. Magn.*, *28* (5) (1992) 2560.

13 W. Gong and G. C. Hadjipanayis, *IEEE Trans. Magn.*, *28* (5) (1992) 2563.

14 L. Schultz, K. Schnitzke, J. Wecker, M. Katter and C. Kuhrt, *J. Appl. Phys.*, *70* (1991) 6339.

15 J. F. Herbst, *Rev. Mod. Phys.*, *63* (1991) 819.

16 B. Hu, H. Li, J. P. Cavigan and J. M. D. Coey, *J. Phys. C*, *1* (1989) 755.

17 Z. W. Li, X. Z. Zhou, A. H. Morrish and Y. C. Yang, *J. Phys. C*, *2* (1990) 4253.

18 J. M. D. Coey, R. Skomski and S. Wirth, *IEEE Trans. Magn.*, *28* (5) (1992) 2332.

19 W. B. Yelon and G. C. Hadjipanayis, *IEEE Trans. Magn.*, *28* (5) (1992) 2332.